

Article

The Optimal Placement and Sizing of Distributed Generation in an Active Distribution Network with Several Soft Open Points

Eshan Karunarathne ^{1,*} , Jagadeesh Pasupuleti ¹, Janaka Ekanayake ² and Dilini Almeida ¹

¹ Institute of Sustainable Energy, Universiti Tenaga Nasional (UNITEN), Kajang 43000, Selangor, Malaysia; jagadeesh@uniten.edu.my (J.P.); dilini@almeida2@gmail.com (D.A.)

² Department of Electrical and Electronic Engineering, University of Peradeniya, Peradeniya 20400, Sri Lanka; jbe@ee.pdn.ac.lk

* Correspondence: eshkaru16@gmail.com

Abstract: A competent methodology based on the active power loss reduction for optimal placement and sizing of distributed generators (DGs) in an active distribution network (ADN) with several soft open points (SOPs) is proposed. A series of SOP combinations are explored to generate different network structures and they are utilized in the optimization framework to identify the possible solutions with minimum power loss under normal network conditions. Furthermore, a generalized methodology to optimize the size and the location of a predefined number of DGs with a predefined number of SOPs is presented. A case study on the modified IEEE 33 bus system with three DGs and five SOPs was conducted and hence the overall network power loss and the voltage improvement were examined. The findings reveal that the system loss of the passive network without SOPs and DGs is reduced by 79.5% using three DGs and five SOPs. In addition, this research work introduces a framework using the DG size and the impedance to the DG integration node, to propose a region where the DGs can be optimally integrated into an ADN that includes several SOPs.

Keywords: active distribution network; distributed generation; optimal planning; particle swarm optimization; soft open points



Citation: Karunarathne, E.; Pasupuleti, J.; Ekanayake, J.; Almeida, D. The Optimal Placement and Sizing of Distributed Generation in an Active Distribution Network with Several Soft Open Points. *Energies* **2021**, *14*, 1084. <https://doi.org/10.3390/en14041084>

Received: 22 January 2021
Accepted: 9 February 2021
Published: 19 February 2021

Publisher's Note: MDPI stays neutral with regard to jurisdictional claims in published maps and institutional affiliations.



Copyright: © 2021 by the authors. Licensee MDPI, Basel, Switzerland. This article is an open access article distributed under the terms and conditions of the Creative Commons Attribution (CC BY) license (<https://creativecommons.org/licenses/by/4.0/>).

1. Introduction

Renewable energy is usually at the top of the spectrum of proposed global developments in any climate change discussion, in order to stave off the worst reverberation of rising temperatures. Renewable energy sources do not produce carbon dioxide, nor do they produce any other greenhouse gas contributing to global warming. In tandem with the need for diminishing carbon emissions, the growing demand for electricity leads to significant renewable energy production. With the latest statistics in the deployment of renewable energy, the cumulative share of renewable energy in power generation would reach 85% in 2050, while non-renewables will account for 15% [1].

It is anticipated that the major share of renewable energy-based power plants will be connected as distributed generators (DGs). They are identified in Ref. [2] as electric power generators or storage typically ranging from few kilowatts to tens of megawatts, which is not a part of a large central power system and is located nearer to the demand. Thus, they reduce the demand for centralized power generation, the losses incurred by lengthy transmission lines, and the voltage instability closer to the feeder endpoints. However, appropriate planning, adaptation, and monitoring of the DGs in the power systems are required to ensure that the grids with a significant portion of intermittent DGs operate effectively. Previous studies have highlighted that the improper siting and sizing of renewables might lead to several challenges in distribution systems. The improper selection of capacity, location, and connection may deteriorate the reliability of distribution networks [3]. Ref. [4] has revealed that problems of stability may result from the incorrect positioning and scaling of DGs. According to Ref. [5], higher DG penetration could not

always guarantee lower line losses and has shown that DG's position and power factor are significant to improve the voltage profile. Furthermore, the non-optimal DG allocation negatively affects overall cost, power quality, and reliability [6]. Ref. [7] has been illustrated the increment in the level of short circuit malfunction due to the inapt location and the size of DGs. Thus, there is an immediate need to determine the optimal DG sizes and locations to minimize the power loss of the system.

2. Related Research

Throughout the scientific literature, different approaches for the challenges of DG allocation and sizing have been identified and could be divided into classical and artificial intelligence algorithms [8]. Optimal scaling and positioning of DGs based on the line voltage stability index were presented in Ref. [9] to reduce the power loss in two different radial distribution systems. In Ref. [10], the authors used a loss sensitivity factor method that is premised on the exact loss equation, to determine the optimum size of a single DG and its corresponding location in three radial IEEE test distribution systems to reduce the total power loss. An analytical approach was analyzed and presented in Ref. [11] to identify the sizes and the siting locations of DGs in IEEE 69 and 33 radial systems to minimize power loss. Ref. [12] employed a loss sensitivity factor based on equivalent current injection for determining the optimum size and location of distributed generation in three radial distribution systems to minimize total power losses. Analytical expressions to ascertain the size and the power factor of a DG, which has the ability to inject active power and reactive power, were proposed in Ref. [13] to achieve the highest loss reduction in a radial distribution system. In Ref. [14], a two-phase methodology incorporated with a siting and capacity planning model for optimally site and size DGs was presented for loss minimization of IEEE 33 and 69 radial distribution systems. Mixed-integer non-linear programming (MINLP) approach was used in Ref. [15] to optimally place and size multiple DGs in IEEE 69 and 118 radial distribution systems to minimize the power losses and the generation cost. Ref. [16] proposed the genetic algorithm (GA) for optimal sizing and positioning of DGs to minimize the power loss of the IEEE 33 and 69 radial distribution systems. In Ref. [17], a methodology for optimal DG allocation and sizing was presented using GA to minimize the power loss to improve the voltage profile and the energy-saving benefit of the IEEE 33 bus system. Moreover, Ref. [18] presented a methodology to optimally locate and size a single DG in a radial distribution system that forms a part of the Egyptian distribution network in the interests of reducing power losses, power flow reduction in critical lines, and the voltage profile improvement. Ref. [19] discussed an artificial bee colony method to determine the optimal DG size, location, and power factor to minimize the total system losses of IEEE 15 and 33 radial distribution systems. The combination of GA and particle swarm optimization (PSO) was used to site and size DGs in Ref. [20] and the objective was to minimize network power losses of IEEE 33 and 69 radial systems. In Ref. [21], artificial bee colony and cuckoo search-based hybrid algorithm was employed to identify the optimal sitting and scaling of DGs for a 30-node radial distribution system, and minimization of the power losses and the improvement of the voltage profile were selected as the objectives of the optimization. Optimal sizing and positioning of DGs to reduce the power loss of IEEE 15 and 33 bus systems were presented in Ref. [22] by using PSO. The authors of Ref. [23] proposed the PSO method to determine the optimal allocation and capacity of DGs for the power loss minimization of the system. For the same radial system, comprehensive learning PSO was utilized for the sizing and placement in Ref. [24] to minimize the total power loss of the system. Ref. [25] suggested multi-leader PSO for optimal placement and sizing of DGs to minimize the power loss without violating system constraints in a radial distribution system.

All the reviewed studies on optimal placement and sizing of DGs to minimize power losses examine the impacts on conventional and standard radial distribution networks with normally open points (NOPs) due to their inherent simplicity and low cost. However, these standard radial distribution networks do not contemplate any interconnections between

radial feeders, which enables power delivery through less loaded feeders. In the event of unplanned, scheduled power failures or a system modification, the network feeders often have to connect to the adjacent feeders by closing NOPs to keep up the reliability by creating alternative electricity supply routes in real active distribution networks (ADNs). In addition, an ADN with closed NOPs would also enhance the power loss reduction, the voltage profile, and the authenticity of the system. Furthermore, the optimal adaptation of DGs could further enrich the afore-mentioned enhanced voltage profiles and loss reduction of the ADNs with closed NOPs.

With the enhancement of power electronic technologies currently available, the possibility of replacing a NOP with a “soft open point (SOP)” has been considered [26,27]. SOP furnishes a fast, dynamic, and continuous active current controlling among ADN feeders for loss minimization, load balancing, and the optimization of the voltage profile. The isolated dc link and the limited short circuit current of this device also enables fast restoration of the supply and immediate isolation of interconnected feeders during faults [28,29]. Consequently, SOPs are able to enhance the operation of ADN by increasing power loss reduction and promote more DG penetration into ADNs. Previous studies have manifested the benefits of SOPs for ADNs with a large capacity of DGs. In Ref. [27], three DGs were connected arbitrarily with the non-optimized sizing to investigate the impact of DG connection for the minimization of power loss and the load balancing of the feeders in an ADN with SOPs. Ref. [30] demonstrated the capability of SOPs in facilitating benefits to an ADN in terms of power loss reduction and voltage improvement by integrating four DGs connected to randomly selected nodes. The network with arbitrarily connected 10 DGs, whose cumulative active power reaches almost 100% of the peak demand, was used in Ref. [31] to investigate the voltage controlling capability of SOPs in ADNs. In Ref. [32], the capability of SOP was analyzed to increase DG integration. However, the locations for DG integration were selected randomly and the scales of DGs were utilized as a percentage penetration by considering a worst-case scenario. Almost all these studies, which are related to the benefits and capabilities of SOPs, and the support on network performance in terms of loss reduction and voltage deviation, have not considered any optimized methodology in placing and sizing of DGs. Furthermore, they consider a test system with only a few SOPs, not all the possible SOP connections, to analyze their contributions.

Therefore, in this paper, the optimal placement and sizing of DGs in ADNs were determined with the intention of active power loss reduction by replacing the NOPs with SOPs. In order to assess the impact of the number of SOPs, all possible combinations of SOPs were utilized to restructure the ADN. All the restructured ADN structures were used to integrate DGs and examined the power loss reduction and voltage profile improvement of the ADN system. The PSO was used to establish the optimal sizes of DGs and the optimal location was identified using a methodology based on the voltage stability index. In addition to the above considerations, one of the major contributions of this research is the demonstration of the generalized approach for the planning of a predefined number of DGs in a distribution system with a predefined number of SOPs. Moreover, the most feasible region for the sizing and placement of DGs to obtain minimum loss of the network is recognized in terms of “DG momentum” that uses the DG size and the minimum impedance from the substation to the integration node.

The remainder of the paper is arranged as follows: Section 3 illustrates network structuring using the SOPs and the power loss of the SOPs. Section 4 demonstrates the problem formulation including the objective function and the involved constraints. The framework of the optimization process used for the optimal siting and scaling of DGs, which is based on the voltage stability index and the PSO algorithm, is presented in Section 5. Section 6 illustrates the generalized methodology for the siting and sizing of predefined number DGs and SOPs in a distribution system. The case study and the findings are given in Sections 7 and 8 to illustrate the effectiveness of the proposed method in terms of loss reduction and voltage improvement using the IEEE 33 bus system. Discussion of the findings is presented in Section 9, and Finally, the conclusions are drawn in Section 10.

3. Network Structuring

3.1. SOP Combinations

The ADNs have points where the nearby network feeders can be connected using SOPs, which can generate different structures of networks. In turn, multiple SOPs can be used in an ADN. In this study, different network structures are generated considering different SOP combinations. If the number of SOPs that can be adopted by an ADN is Y and the number of SOPs in use at a time is $W(\leq Y)$, the number of available network structures ($C_{W(Y)}$) can be expressed as in Equation (1),

$$C_{W(Y)} = C_W^Y + C_{W-1}^Y + \dots + C_2^Y + C_1^Y + C_0^Y = \sum_{i=0}^W C_i^Y; \text{ for } i = 0, 1, 2, \dots, W \quad (1)$$

where $C_W^Y = \frac{Y!}{W!(Y-W)!}$. For example, if the overall number of SOPs linked to the system is 5 and the number of SOPs that could be used at a time is 3, then the number of modified network structures that could be developed ($C_{3(5)}$) is 10. The SOPs used in the possible 10 number of network structures are shown in Figure 1. Its columns and rows represent the network structure number and the SOP number respectively. The yellow color buttons are the enabled SOPs and the gray color buttons are the disabled SOPs of the network structure where a disabled SOP means the SOP, which is controlled to be switched off. Accordingly, the total number of network structures that can be developed using Y SOPs is represented by C_Y .

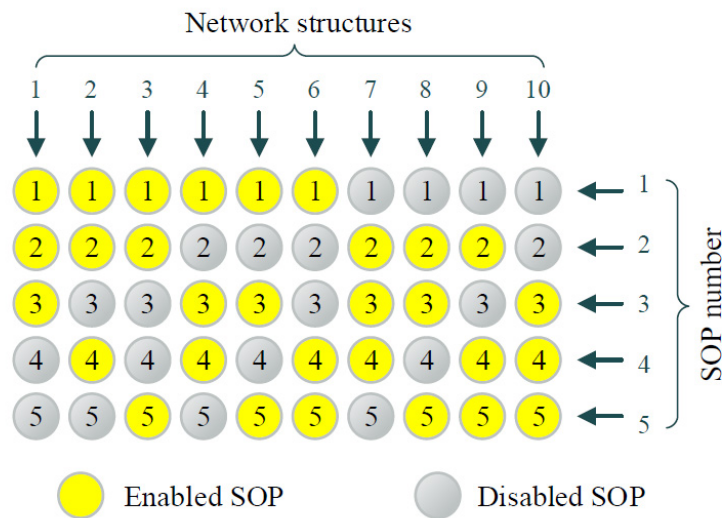


Figure 1. Possible network structures developed using three soft open points (SOPs).

3.2. Power Losses of the SOPs in Network Structures

The SOP could be realized in various topologies, and in this study, the topology of back-to-back voltage source converter (B2B-VSC) was assumed and exploited. An ADN, connecting two adjacent feeders 1 and 2 (with m and n nodes) using an SOP is depicted in Figure 2. B2B-VSC could function in all four quadrants and the active power flow can be supervised expeditiously with more accuracy [29]. In addition, independent reactive power capacities could be set to both terminals. The active power flow at SOP terminals has been included in the power flow computation and the operational delimitations of the SOP are,

$$P_{m,1} = P_{con1} + P_{loss(m1,con1)} \quad (2)$$

$$P_{n,2} = P_{con2} + P_{loss(n2,con2)} \quad (3)$$

where P_{con_1} and P_{con_2} are the active power flow through the two VSCs and $P_{loss(m_1,con_1)}$ and $P_{loss(n_2,con_2)}$ are the power losses between bus $(m, 1)$ and VSC₁, bus $(n, 2)$ and VSC₂, respectively. The exchange of active power between the two VSCs are constrained by,

$$P_{con_1} + P_{con_2} + P_{loss_VSC_1} + P_{loss_VSC_2} = 0 \tag{4}$$

$$P_{loss_VSC_1} = K_{VSC_1} * S_{VSC_1} \tag{5}$$

$$P_{loss_VSC_2} = K_{VSC_2} * S_{VSC_2} \tag{6}$$

where $P_{loss_VSC_1}$ and $P_{loss_VSC_2}$ are the power losses of two VSCs, and K_{VSC_1} and K_{VSC_2} are the loss coefficients of the SOPs, while S_{VSC_1} and S_{VSC_2} are the capacity limits of the SOPs. Typically, the loss coefficients equate to 0.2% [27] and the power losses in SOPs could be overlooked relative to the power losses in the entire ADN. Therefore, Equation (4) can be simplified as,

$$P_{con_1} = -P_{con_2}. \tag{7}$$

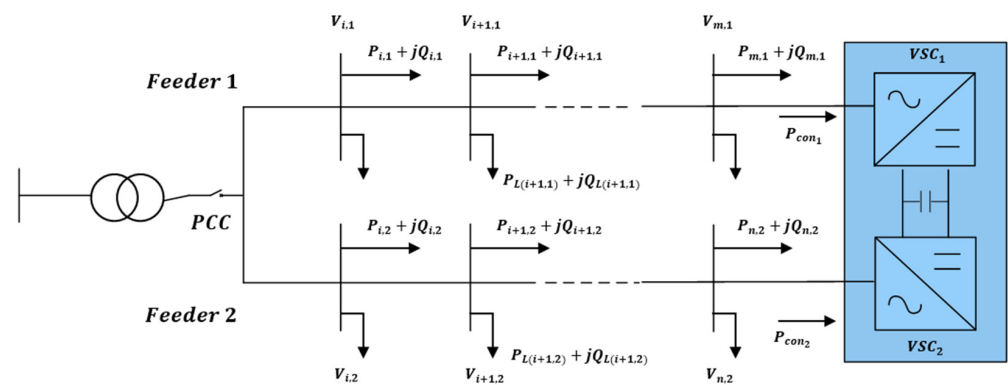


Figure 2. A simple active distribution network (ADN) with an SOP.

It indicates that the injected power from one terminal leaves from the other terminal without a power loss. After this mathematical demonstration, SOP devices with zero internal power losses and zero reactive power supporting capability were considered throughout the study.

4. Problem Formulation

In order to achieve higher efficiency in the power system, the real power loss has to be reduced to the maximum possible level. Thus, the objective of this optimization process was aimed to minimize the overall active power loss. Branch currents and the resistances were utilized to compute the system’s active power loss. Equation (8) mathematically expresses the objective function.

$$\text{Minimize } f = \sum_{m=1}^M P_{loss,m} = \sum_{m=1}^M I_m^2 \times R_m ; \text{ for } m = 1, 2, 3 \dots M \tag{8}$$

where $P_{loss,m}$, I_m , R_m , and M are the active power loss of the m th branch, the flowing current of the m th branch, the resistance of the m th branch, and the total number of branches in the ADN, respectively. This objective function was subjected to the voltage, thermal, DG capacity, and nodal power balance constraints as in Equations (9)–(13).

$$|\underline{V}| \leq V_n \leq |\overline{V}| ; n \in [1, 2 \dots N] \tag{9}$$

$$I_m \leq I_{rated} ; m \in [1, 2 \dots M] \tag{10}$$

$$0 \leq \sum_{n=1}^N P_{DG,n} \leq \sum_{n=1}^N P_{L,n}; \text{ for } n = [1, 2, 3 \dots N] \tag{11}$$

$$\sum_{j \in \phi(i)} (P_{ji} - I_{br,ji}^2 R_{ji}) + P_{DG,i} - P_{L,i} = \sum_{k \in \psi(i)} P_{ik}; i, j, k \in [1, 2, 3 \dots N] \tag{12}$$

$$\sum_{j \in \phi(i)} (Q_{ji} - I_{br,ji}^2 X_{ji}) - Q_{L,i} = \sum_{k \in \psi(i)} Q_{ik}; i, j, k \in [1, 2, 3 \dots N] \tag{13}$$

where $N, \underline{V}, \bar{V}, I_{rated}, \sum P_{DG}, \sum P_L$ are the total number of nodes, lower voltage statutory limit, upper voltage statutory limit, maximum rated branch current, total connected DG size, and total connected load size, respectively. In Equations (12) and (13), $j \in \phi(i)$ denotes all the parental nodes of i th node and $k \in \psi(i)$ indicates all children nodes of i th node. ji and ik implies the directions of the current flow. R_{ji}, X_{ji} and $I_{br,ji}$ are the resistance, the reactance, and the current flowing through the branch that links i th and j th nodes. $P_{DG,i}, P_{L,i}$ are the injection of the active power at i^{th} node and the attached active load at i th node respectively. In the same way, the notations with Q represents the terms related to reactive power.

In order to accomplish the minimization of the objective function while satisfying the constraints in Equations (9)–(13), the penalty functions were incorporated. Consequently, the optimal solution remains within the allowable regions that were defined by the constraints. To implement, an aggregated penalty was levied on the solutions in the cases where the incorporated constraints have not been satisfied. Accordingly, the objective function in Equation (8) was revised and the modified (penalized) objective function (f_p) is given by,

$$f_p = \sum_{m=1}^M P_{loss,m} + K \left(\sum_{n=1}^N V_{p,n} + \sum_{m=1}^M T_{p,m} + DG_p + PB_p \right) \tag{14}$$

where:

$$V_{p,n} = \begin{cases} |V_n - \underline{V}| & ; V_n < \underline{V} \\ 0 & ; \underline{V} \leq V_n \leq \bar{V} \\ V_n - \bar{V} & ; V_n > \bar{V} \end{cases} \text{ for } n = 1, 2, 3 \dots N \tag{15}$$

$$T_{p,m} = \begin{cases} \left(\frac{I_m - I_{rated}}{I_{rated}} \right) & ; I_m > I_{rated} \\ 0 & ; I_m \leq I_{rated} \end{cases} \text{ for } m = 1, 2, 3 \dots M \tag{16}$$

$$DG_p = \begin{cases} 1 & ; \sum_{n=1}^N P_{DG,n} > \sum_{n=1}^N P_{L,n} \\ 0 & ; \sum_{n=1}^N P_{DG,n} \leq \sum_{n=1}^N P_{L,n} \end{cases} \text{ for } n = 1, 2, 3 \dots N \tag{17}$$

$$PB_p = \begin{cases} 1 & ; \text{LHS (12)} \neq \text{RHS (12)} \cup \text{LHS (13)} \neq \text{RHS (13)} \\ 0 & ; \text{LHS (12)} = \text{RHS (12)} \cap \text{LHS (13)} = \text{RHS (13)} \end{cases} \tag{18}$$

$K, V_{p,n}, T_{p,m}, DG_p, PB_p$ are the penalty constant, voltage limit, thermal limit, DG capacity, and nodal power balance penalty functions.

5. Optimization Framework

5.1. Optimal Placement of DGs

The research studies related to the optimal allocation of DGs can split into two major categories [33]. The first category randomly identifies the optimal sitting positions and the second category employs an index to determine the best-suited position for the DG integration. One of the common indexes for determining the weakest node in the system is the voltage stability index (VSI) [34]. However, it is not feasible to address the necessity in locations for the integration of simultaneous multiple DGs because only a single node of integration is given by the second method. Thus, a VSI-based approach was employed to find the suitable nominee locations that allow the simultaneous integration of DGs in

this study. In comparison, this approach will enhance the network voltage stability more than the random selection of nodes for the integration of DGs. According to the single line diagram (SLD) shown in Figure 3, the VSI term was calculated as below.

$$VSI = 2|V_l|^2|V_k|_2 - |V_l|_4 - 2|V_l|^2\{P_l R_{kl} + Q_l X_{kl}\} - |z_{kl}|^2\{P_l^2 + Q_l^2\} \quad (19)$$

where $|z_{kl}|^2 = \{R_{kl}^2 + X_{kl}^2\}$. VSI measures the proximity of nodes to cause a voltage collapse in an ADN. Low VSI values are more sensitive to collapse. Therefore, the nodes with VSI values that are lower than a pre-defined value (VSI_{lim}) are counted as the nominee nodes in this study.

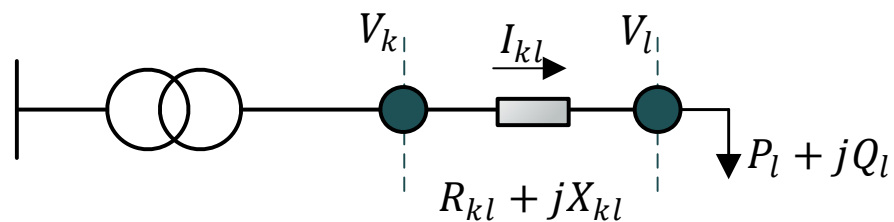


Figure 3. Single line diagram (SLD) of a radial system with two nodes.

The steps of the algorithm used for identifying the nominee locations for the integration of DGs are shown in Figure 4. Initially, the power flow analysis is conducted and the VSI values are calculated. The nominee nodes, which are selected according to the calculated VSI values (N_N -green color nodes), are utilized to produce the sets of sites for the integration and every produced set of sites have different nodes. Finally, the produced nominee node sets are sent to the optimization procedure. In this approach, the capability of selecting multiple locations is enabled compared to other methods that select a single node. Furthermore, this would benefit in alleviating the search space of DG integrating nodes. This procedure is graphically demonstrated in Figure 4.

5.2. Optimal Sizing of DGs

Various algorithms have been used in previous works to determine the optimal sizing of DGs. However, most of them have limitations and they are described in Table 1 for selected algorithms.

Table 1. Limitations of different algorithms used for optimal sizing of distributed generators (DGs).

| Algorithm | Limitations |
|-------------------------|---|
| Analytical methods | Do not consider convergence and precision errors that could occur when solving complex problems. |
| GA | Computationally inefficient and effortlessly achieve the premature convergence. The number of iterations used to reach the optimal solution is higher than PSO. |
| Ant Colony Optimization | The convergence time is uncertain and the theoretical analysis is difficult. |
| Tabu Search | A large number of iterations needed than PSO, time-consuming, numerically inefficient. |
| Artificial Bee Colony | Easily stuck in local optima when solving complex problems. |

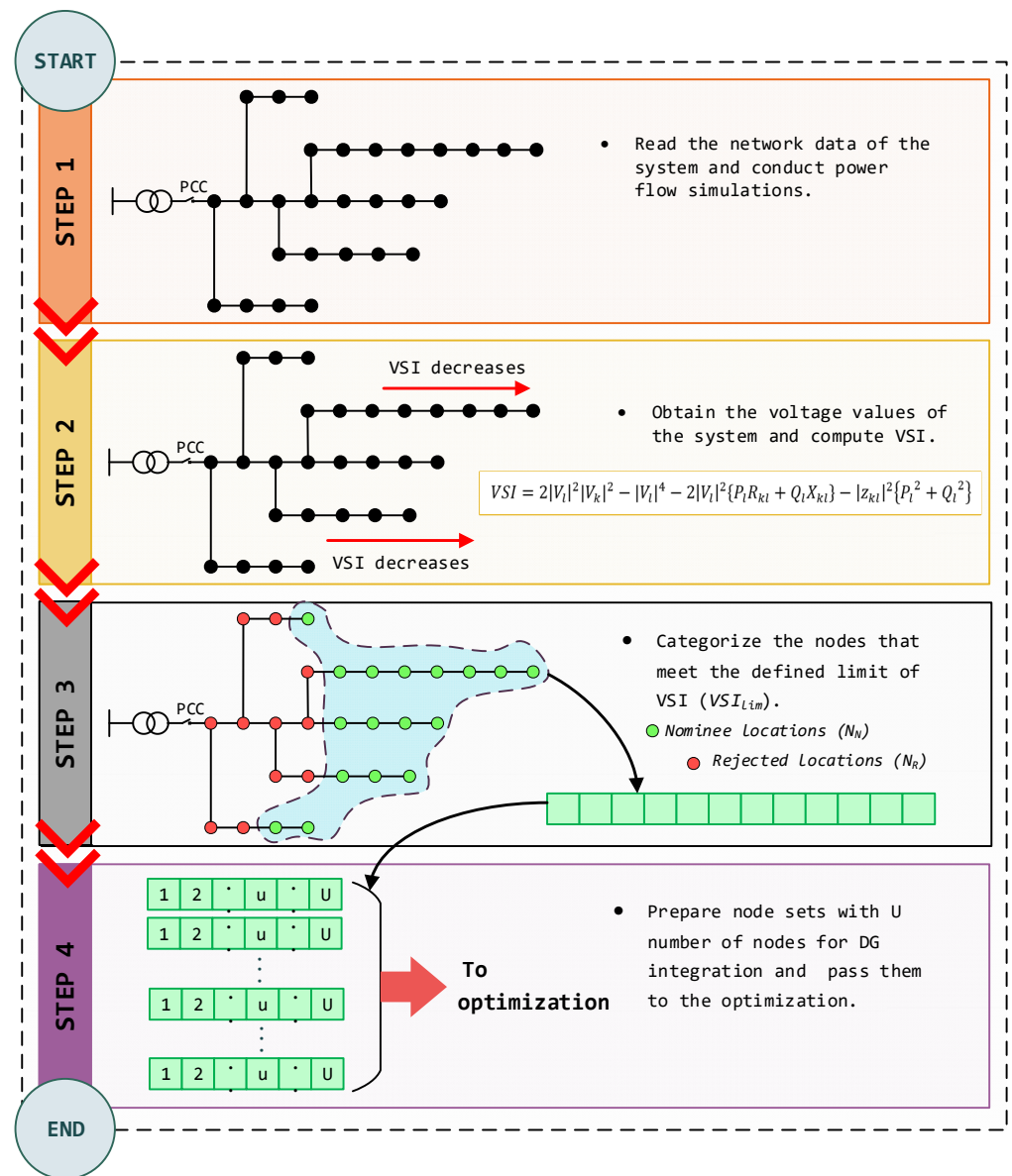


Figure 4. Identifying nominee nodes using a voltage stability index (VSI)-based method-Algorithm 1.

In the PSO algorithm, a lesser number of iterations are used, and consequently, the computational burden is extremely lower compared to the other optimization algorithms. In addition, preconditions including differentiability or continuity of the objective functions and mutation processes do not apply to the PSO algorithm. Comparatively, the implementation and the usage are straightforward in PSO. Furthermore, the PSO algorithm has the capability of solving large-scale non-linear problems, and it is one of the most promising techniques in terms of solution and convergence [35,36]. Considering the above advantages, the PSO algorithm was chosen.

The PSO algorithm is an evolutionary algorithm, and it was proposed by Kennedy and Eberhart in 1995 [37]. It is based on the behavior of the birds in a flock. This algorithm operates to explore suitable areas in a multi-dimensional environment to locate the optimal solution. The decision variables are indicated by the dimension of the particle. The PSO algorithm conducts the searching process via a swarm of particles and updates the velocity

(V_i^d) and the position (X_i^d) of the particles in every iteration according to Equations (20) and (21).

$$V_{i(updated)}^d \leftarrow \omega_k V_i^d + c_1 rand_i^d (pbest_i^d - X_i^d) + c_2 rand_i^d (gbest^d - X_i^d) \quad (20)$$

$$X_{i(updated)}^d \leftarrow X_i^d + V_{i(updated)}^d \quad (21)$$

where X_i^d and V_i^d are the position and velocity of d th dimension of i th particle. $pbest_i^d$ and $gbest^d$ are the i th particle's personal best and the global best of the entire swarm, respectively. c_1 and c_2 are positive constants and defined as acceleration coefficients. A random number is indicated by $rand_i^d$, which is in between 0–1. ω is named as the inertia weight. It is used to balance the ability of global and local exploration and in each iteration, it linearly varies according to Equation (22) in between ω_{min} and ω_{max} values.

$$\omega = \frac{(\omega_{max} - \omega_{min})}{ITE_{max}} \times ite \quad (22)$$

where ITE_{max} and ite are the maximum number of iterations and the current iteration respectively. Every particle in the swarm tries to enhance the performance of the algorithm by updating its position, velocity, and other parameters in various acceptable regions.

In this study, the particles' initial positions were produced taking into account the total allowed DG size that could be integrated into the distribution system. The main reason behind this was to alleviate the computational time than that of a random selection of initial positions. Therefore, the positions of the particles were initialized according to Equation (23).

$$\sum_{d=1}^D x_i^d \leq \sum_{n=1}^N P_{L,n} \text{ for } \forall i \in s \quad (23)$$

where D is the i th particle's dimension and s is the number of the particles. Figure 5 depicts the complete flow chart used for the optimal sizing of DGs in this study. Table 2 indicates the parameter values used in the PSO algorithm. The inertia weight bounds, cognitive coefficient, social coefficient, and the number of iterations were selected by considering the values used in previous studies.

Table 2. The PSO algorithm parameters for the optimal sizing of DGs.

| Parameter | Value |
|--|-----------|
| Swarm size (s) | 500 |
| Number of dimensions in a particle (D) | 3 |
| Maximum number of runs (R) | 10 |
| Maximum number of Iterations (ITE_{max}) | 10^3 |
| Upper bound of the inertia weight (ω_{max}) | 0.9 |
| Lower bound of the inertia weight (ω_{min}) | 0.4 |
| Cognitive coefficient (C_1) | 2 |
| Social coefficient (C_2) | 2 |
| Upper voltage limit (\bar{V}) | 1.05 p.u. |
| Lower voltage limit (\underline{V}) | 0.95 p.u. |
| Maximum Thermal limit (I_{rated}) | 300 A |

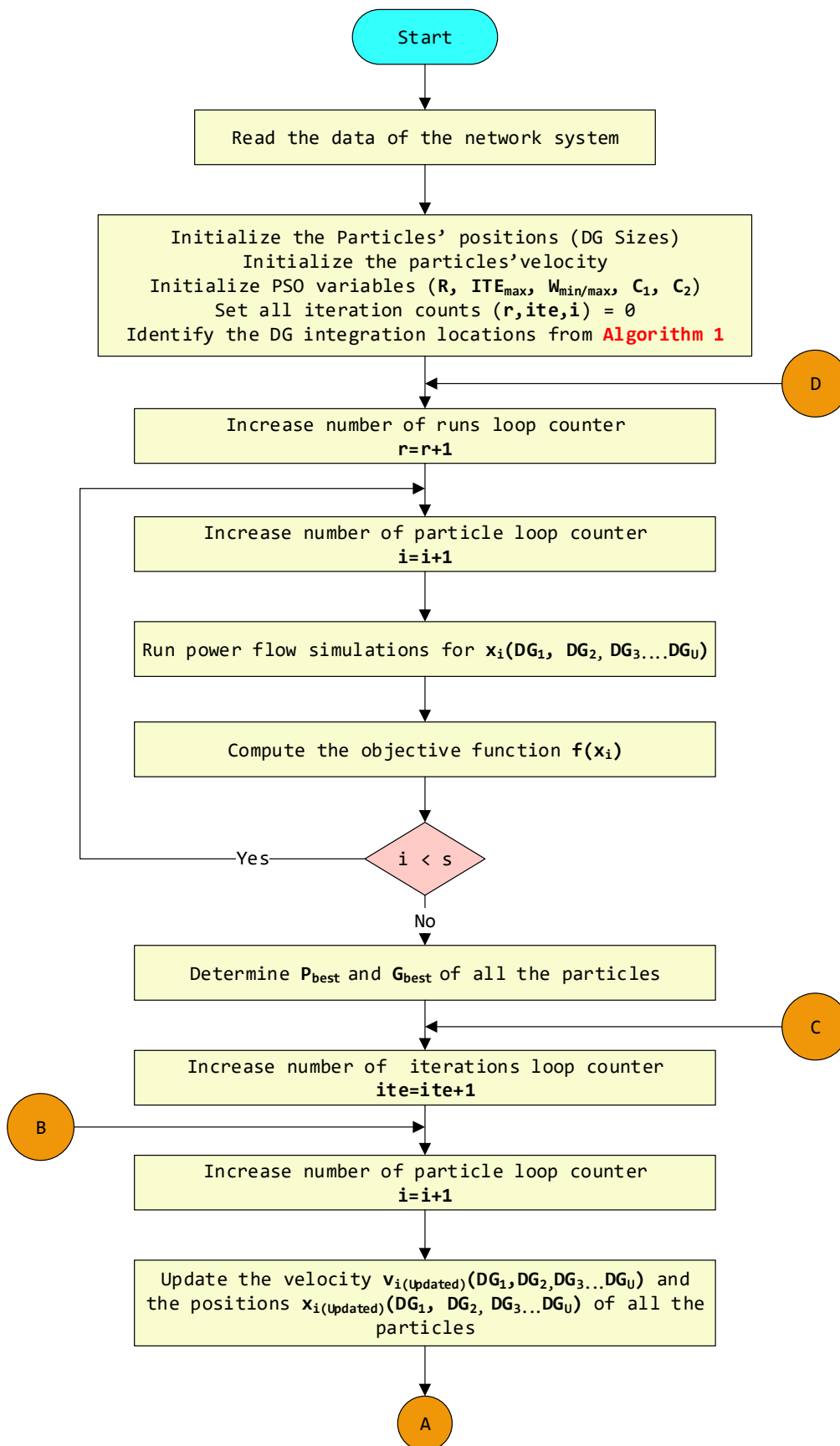


Figure 5. Cont.

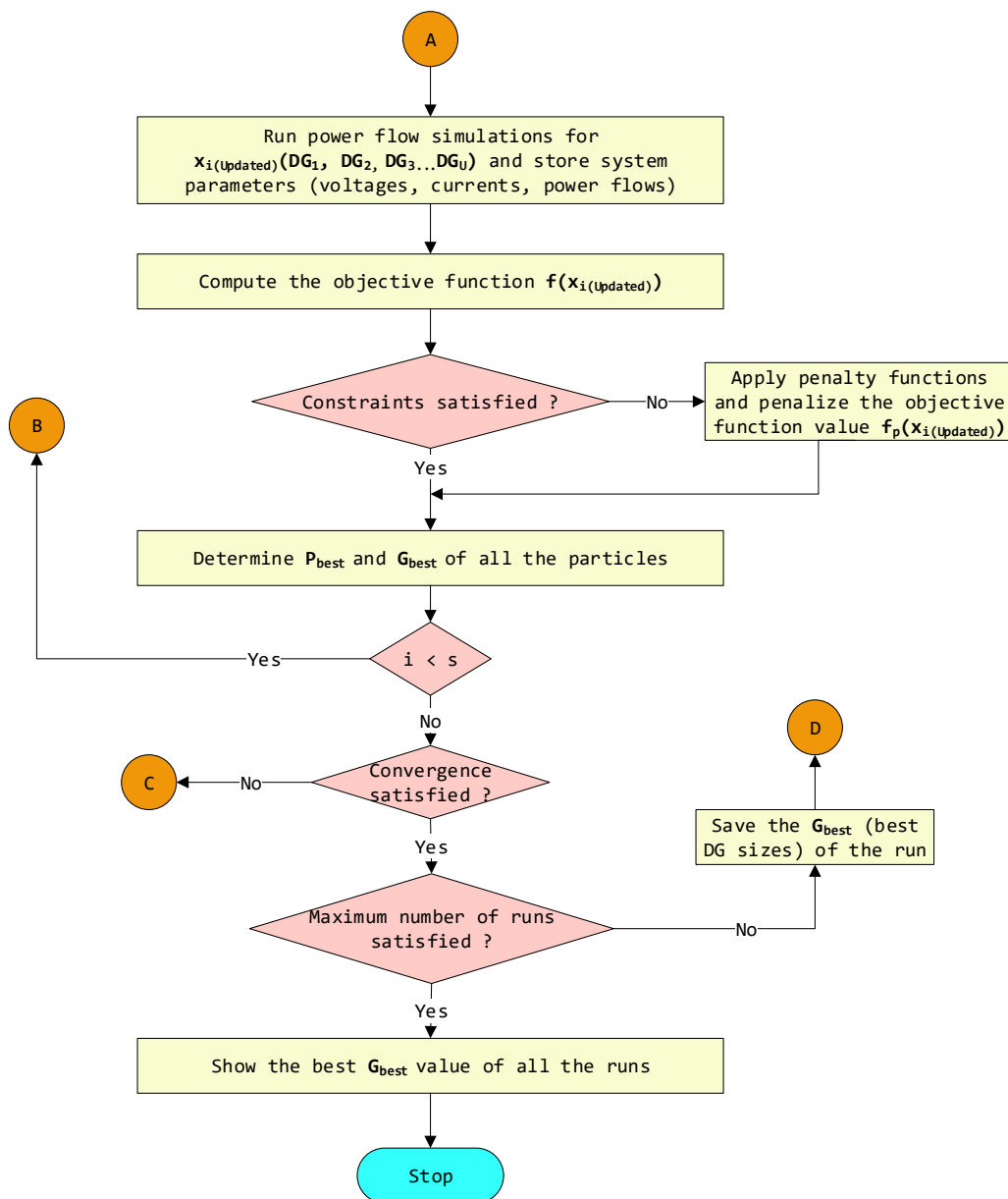


Figure 5. Flow chart of optimal sizing of DGs utilizing the particle swarm optimization (PSO) algorithm—Algorithm 2.

6. Generalized Methodology

As shown in Figure 6, the optimization process determines the optimal locations and sizes of U number of DGs in various modified network structures by deploying W number of SOPs at different locations ($C_{W(Y)}$ - possible number of modified network structures using W out of Y SOPs).

Initially, the networks were modified according to the number of SOPs and their locations. Thereafter, the modified networks were stored. Parallely, the nominee locations for DG placements were identified using the original network by Algorithm 1 and passed to the optimization process. The optimization process was applied to all the developed structures ($C_{W(Y)}$) and each optimization process includes R number of optimization runs. s number of particles were utilized to perform each run and the total number of particles used for a network structure is $R.s$ and they are U dimensional (i.e., dimension = number of DGs).

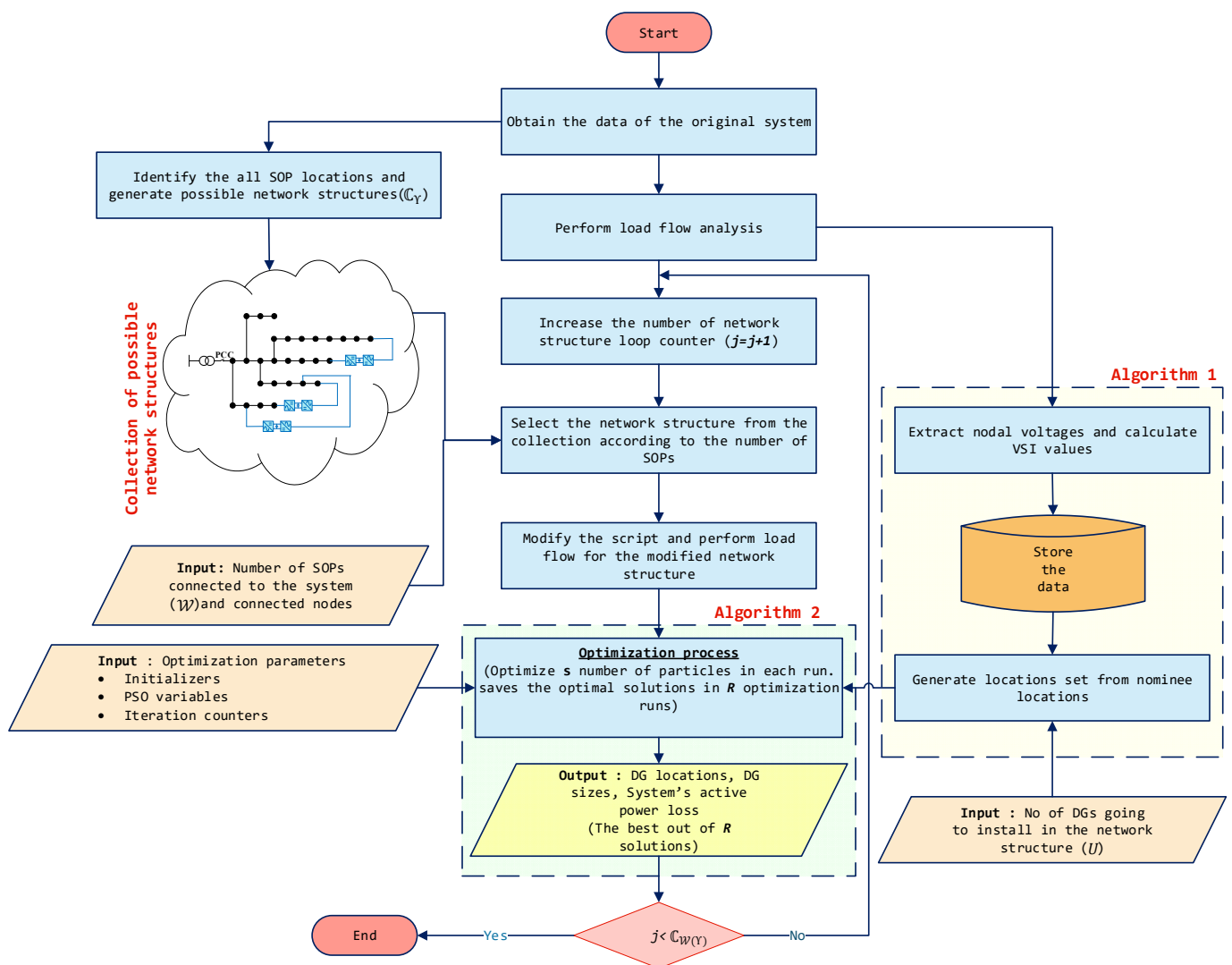


Figure 6. Flow chart of the generalized methodology.

After a large number of power flow simulations, the optimization process gives out R number of minimum losses, DG location sets, and DG size sets for each network structure. Then, the minimum loss out of R runs (i.e., the best optimal solution) was obtained and the corresponding run with the minimum loss was established as the best run. The respective location set and the DG size set were considered as the best-optimized solutions for the corresponding network structure. In the entire simulation process, all network structures use $R \cdot C_{W(Y)}$ number of particles and out of them, the optimization algorithm gives $C_{W(Y)}$ number of particles as the best solutions for all $C_{W(Y)}$ network structures. The best solutions consist of U number of DG sizes and locations and the active power loss of each network. Figure 6 clearly demonstrates the described optimization process for a $C_{W(Y)}$ number of modified network structures.

7. Case Study

The modified IEEE 33 bus system was employed for the simulations of this paper [38]. The network is rated at 12.66 kV voltage, with a total demand of 3.715 MW and 2.3 Mvar. It was assumed that the system is three-phase and balanced. The maximum branch thermal limit value was set to 6.6 MVA, and it represents the maximum flow of current equals 300 A. For all the nodes, the upper and lower voltage statutory limits were fixed to 1.05 p.u. and 0.95 p.u. in compliance with the standard medium-voltage statutory limits. The NOPs were chosen as the nominee sites for the deployment of SOPs, (i.e., the switches between

buses 8 and 21 (SOP 1), 9 and 15 (SOP 2), 12 and 22 (SOP 3), 18 and 33 (SOP 4), 25 and 29 (SOP 5), as shown in Figure 7).

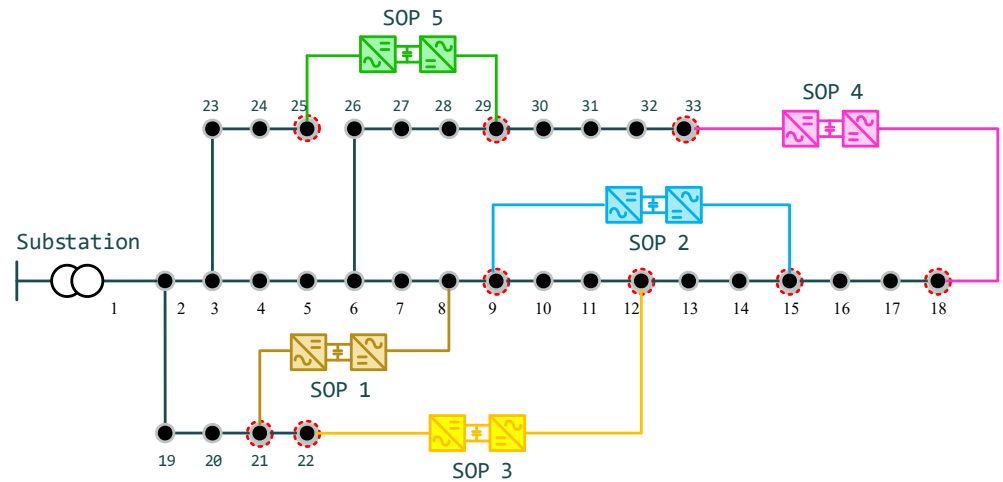


Figure 7. SLD of the modified IEEE 33 bus system with five SOPs.

8. Results

The proposed generalized methodology was validated on the modified IEEE 33 bus system shown in Figure 7. A scenario with three DGs ($U = 3$) was simulated for quantifying the performance improvement of ADNs with SOPs and optimized DG integration. In the presence of five SOPs ($Y = 5$) in a passive network system, 32 different network structures ($C_5 = 32$) could be developed using different SOP combinations as presented in the button matrix in Figure 8. This figure shows the SOP combinations of each network structure and represents the enabled and disabled SOPs by colored and non-colored buttons, respectively. The first network structure does not have any SOPs and the last network structure (i.e., 32nd structure) has all the SOPs.

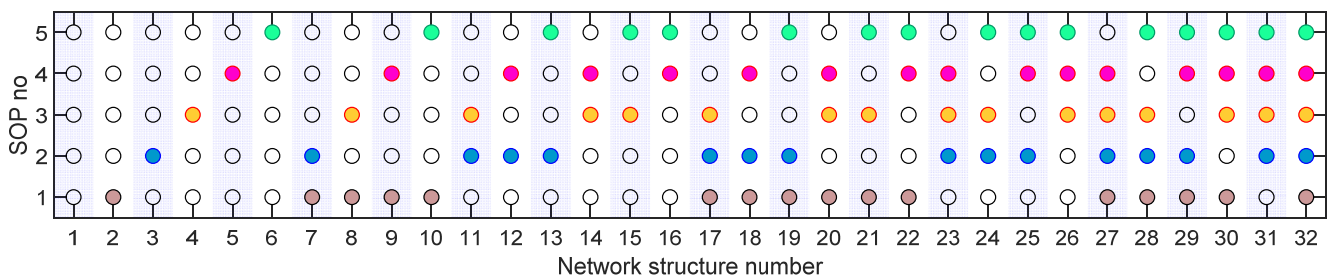


Figure 8. The button matrix of SOP combinations.

The VSI was used to identify the set of candidate locations of the passive system for DG integration. It was ensured that this set of candidate locations comprises VSI values that are less than 0.9 ($VSI_{lim} = 0.9$) because the nodes of the passive network with $VSI < 0.9$ violate the lower voltage limit. From VSI, it was identified that nodes 1–5 and 19–23 are not candidates for DG connections.

The sizing of the DGs was undertaken by the PSO algorithm. For each network structure, 10 optimization simulations ($R = 10$) were performed utilizing 5000 particles ($R.s = 5000$). In this simulation process, 160,000 particles ($R.s. C_5$) were initially used for all 32 network structures and finally, the best 32 particles (i.e., the optimal solution for each network structure) were selected through the optimization for all 32 structures. As an example, the cumulative DG sizes and the cumulative impedance of possible solutions that were obtained from the best run of the fourth network structure were plotted with the

corresponding active power loss as shown in Figure 9. The optimal solution is shown with a red star.

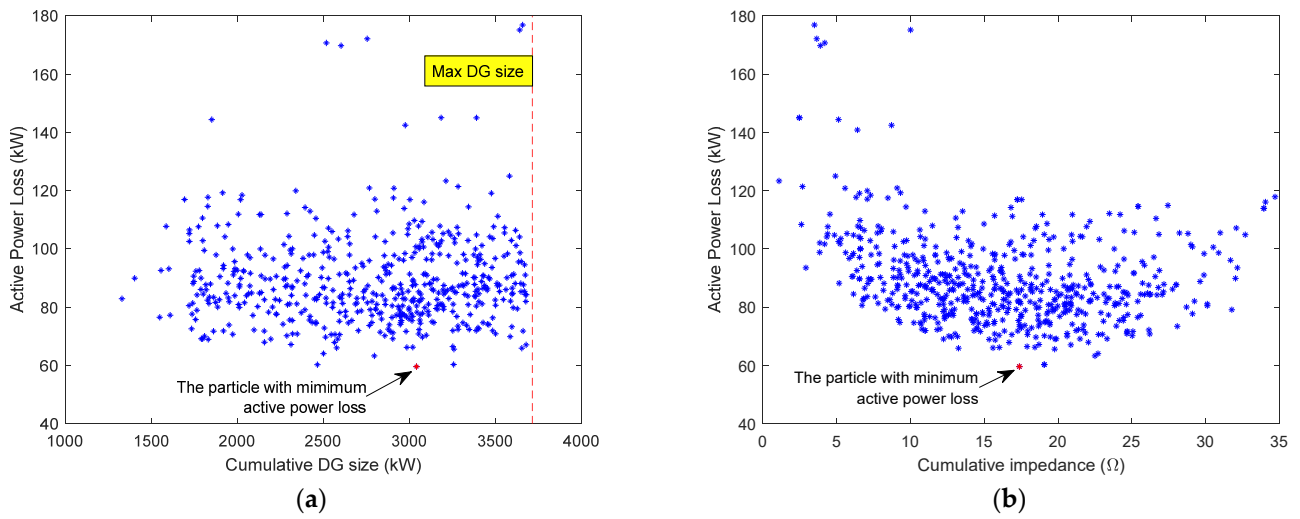


Figure 9. Variation of active power loss with (a) the cumulative DG sizes and (b) the cumulative impedance of possible solutions that were obtained from the best run of the fourth network structure.

The optimal solutions obtained for the DG locations and sizes from the optimization process for all the network structures are graphically presented in Figure 10. The DG locations are shown in blue color dots. The variation of the minimum active power losses that was identified from the best possible solutions (i.e., the optimal solution) of the best runs in each network structure is plotted in Figure 11, and the minimum and mean voltage variations of all the network structures are shown in Figure 12.

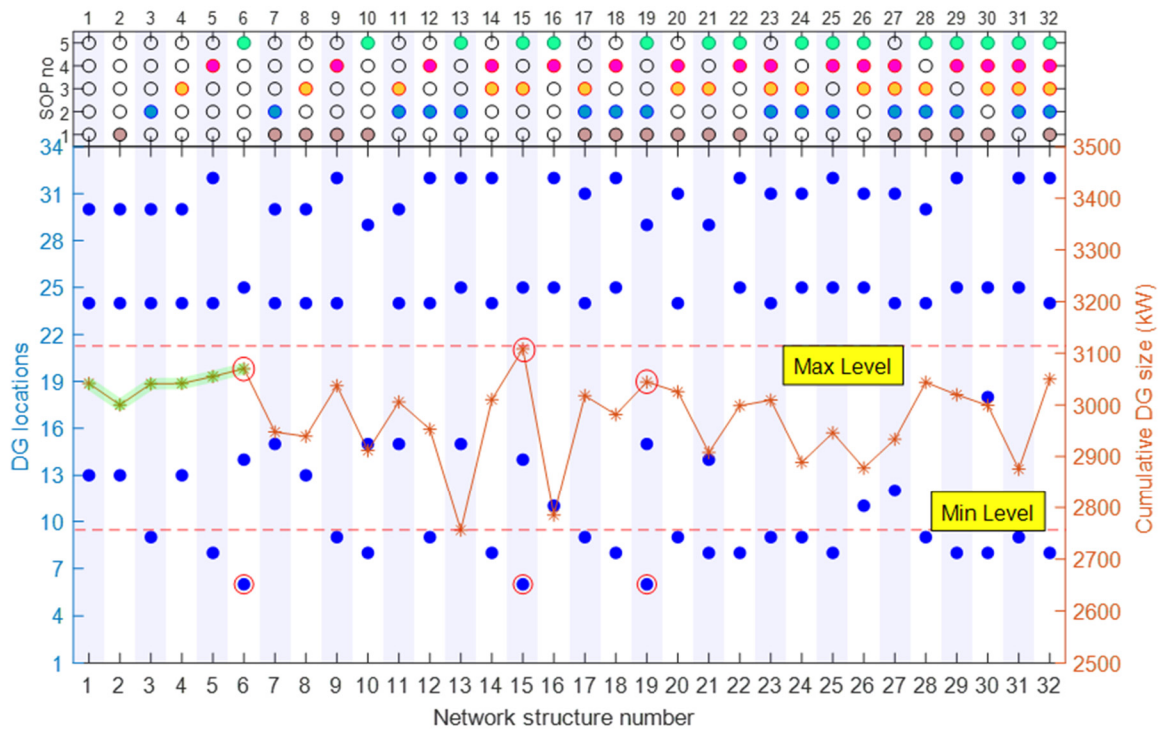


Figure 10. DG locations and the cumulative DG sizes for all the network structures.

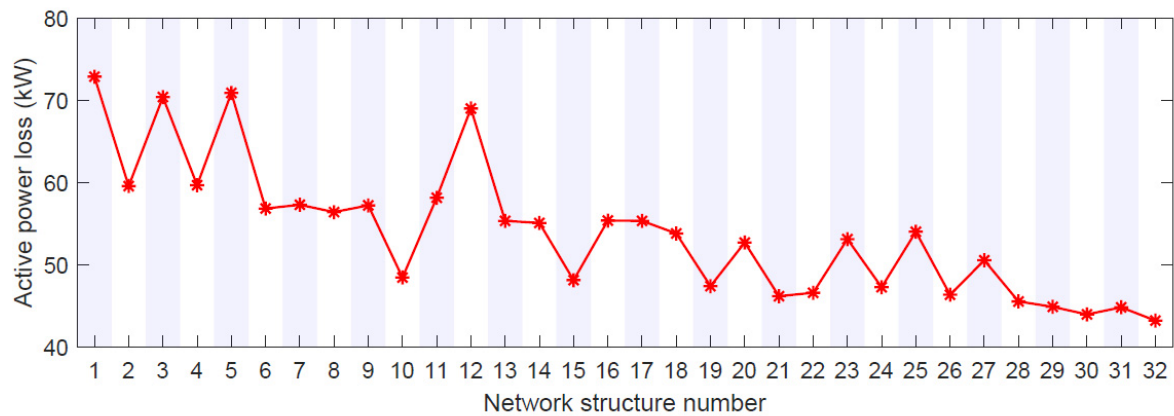


Figure 11. Variation of the active power loss of all the network structures.

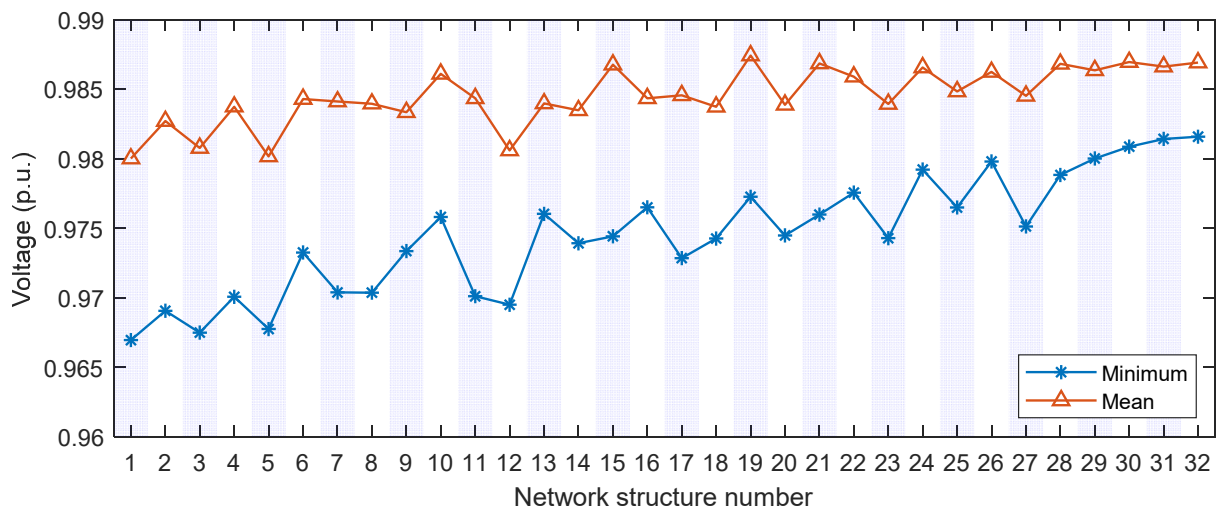


Figure 12. Variation of minimum and mean voltage of all the network structures.

9. Discussion

In this analysis, the simulations were centered on steady-state power flows at the peak loading condition. The peak loading condition had a substantial impact on the system's power loss in comparison with other loading conditions due to the high-power flows throughout the distribution system.

As shown in Table 3, the optimum cumulative DG sizes conducted to the IEEE 33 bus system were less than the total load connected to the system. Thus, in this study, the maximum permissible cumulative DG size was limited to the total connected load demand. This enables to draw an output closer to the optimal value, alleviate the computational burden of the algorithm, and establish the zero reverse power flow towards the grid in all network structures at peak loading conditions. However, reverse power flows could occur during minimum loading conditions with the optimum sizing of DGs [39].

As per the example shown in Figure 9a, the minimum loss (i.e., the optimal solution) is recorded as 59.1 kW with a cumulative DG size of 3040 kW. It is represented by a red color star in Figure 9a. Furthermore, a single particle in that figure consists of the cumulative value of DG size and does not provide any information about the locations of three DGs connected. Therefore, the overall impedances from the substation node (N^s) to the DG integration nodes were computed by taking the shortest impedance path when there were SOPs in the network. Accordingly, Figure 9b presents the variation of the system's active power loss with the resulting cumulative impedance of the locations of the same possible solutions. A clear "U trajectory" could be observed from the two parameters emphasizing

a decrement of active power loss during the initial impedance values and an increment of active power loss after a certain impedance value. The same particle that is identified as the minimum loss in Figure 9a is also recognized in Figure 9b, and it is represented in a red color star.

Table 3. Comparison of loss reductions of different algorithms in IEEE 33 bus system with three DGs.

| Algorithm/Year | Total Load (kW) | Total DG Size (kW) | Connected Nodes | Loss Reduction (%) |
|----------------------------------|-----------------|--------------------|-----------------|--------------------|
| PSO (this paper - 1st structure) | 3715 | 3040.00 | 13, 30, 24 | 65.30 |
| CSCA/2020 [40] | | 2916.55 | 13, 24, 30 | 64.50 |
| TM/2017 [41] | | 2879.50 | 15, 33, 26 | 49.52 |
| MOTA/2017 [41] | | 3280.00 | 7, 30, 14 | 52.40 |
| BA/2016 [42] | | 2721.60 | 15, 30, 25 | 64.42 |
| HSA/2013 [43] | | 2688.60 | 18, 33, 17 | 52.26 |

As described above, the best DG sizes and the best locations (i.e., the optimal solution), which are depicted by the red color particles in Figure 9a,b, were obtained from the optimization process for all the network structures and graphically presented in Figure 10. It is associated with a button matrix that depicts the enabled and disabled SOPs in each network structure. It could be seen that the cumulative DG sizes for all the network structures were within 3110 kW (Max level) and 2750 kW (Min level). It was identified that the total DG sizes were comparatively higher when one of the DGs was located in the first half of the longest lateral that includes nodes 1 to 9 (i.e., closer to the substation). The solutions that offer the first three maximum cumulative DG sizes and the corresponding DG locations that were positioned nearer to the substation (at node 6) were circled in red color. In addition, it could clearly have higher DG sizes when zero or a single SOP was involved in the network structure (1–6 network structures), and they were highlighted in green color. The main reason behind this was the long power flow path due to the involvement of a fewer number of SOPs. Moreover, the DGs were tended to site at the feeder end nodes of most of the network structures (i.e., 24–25 and 29–32 nodes). Furthermore, the DGs were not sited on the restricted nodes where VSI > 0.9 (i.e., 1–5, 19–23 nodes). When all three DGs were placed at the nodes closer to the feeder ends, the DG sizes were varied in the middle of the maximum range.

The variations of the minimum active power losses that were identified from the best possible solutions (i.e., the optimized solution) of the best runs in each network structure are plotted in Figure 1, and it is in-line with the same button matrix for easy understanding of enabled and disabled SOPs in each network structure. The results clearly show an alleviation of losses by increasing the number of SOPs. According to the third, fifth, and twelfth network structures in Figure 11, it could be seen that the second and fourth SOPs contribute less to reducing loss when they were alone in the network structures. The minimum active power loss was recorded as 43.167 kW with five SOPs (32nd structure) and it corresponds to a power loss reduction of 79.5% compared to the passive network loss without SOPs and DGs, which is 210 kW. Similarly, the maximum loss was recorded as 72.85 kW with no SOPs (1st structure) and it corresponds to a power loss reduction of 65.3% compared to the passive network loss.

Based on the recent research works, the active power loss reductions in IEEE 33 bus system obtained from various optimization algorithms when integrating three DGs are given in Table 3.

Comparing the listed data in Table 3, the PSO is capable of providing the maximum loss reduction with three DGs compared to the other optimization algorithms. According to the best of the authors' knowledge, the optimal placement and sizing of DGs in an ADN with several SOPs have not been investigated in the existing literature.

Figure 12 shows the minimum and mean voltage variations of all the network structures. The minimum voltage of the passive IEEE 33 bus system was 0.9042 p.u. and it was increased up to 0.9669 with 3DGs (1st structure). It could be seen that the minimum and mean voltages depict an incremental trend with the number of SOPs increases. The highest minimum voltage has shown by the 32nd structure. From the results, it was clear that the lower power losses were influenced by both the DG location and size, and therefore, a new term was defined as “momentum of integrated DGs (M_{DG}),” which could be mathematically expressed as follows:

$$M_{DG}(\text{kW}\Omega) = \sum_{i=1}^U \text{DG size}(\text{kW}) \times \text{Minimum Impedance to the integration node from the substation } (\Omega) \quad (24)$$

where U is the number of integrated DGs into the network structure.

Using the extracted DG sizes and the locations of the 32 network structures, the momentum of integrated DGs was computed for all the possible solutions and it is shown in Figure 13. From this study of the integrating three DGs into the IEEE 33 bus distribution network, it was identified that the momentum of the integrated DGs in all network structures (red stars) varies within the range of $1.4 \times 10^4 \text{ kW}\Omega$ to $1.75 \times 10^4 \text{ kW}\Omega$ to obtain a minimum loss in the corresponding network structure. These momenta values have always ensured the limits of the total DG sizes and impedance values. This can be used as a rule of thumb for a given network so that DG connections can be expedited while ensuring the minimum losses as many utilities are having loss targets to be met.

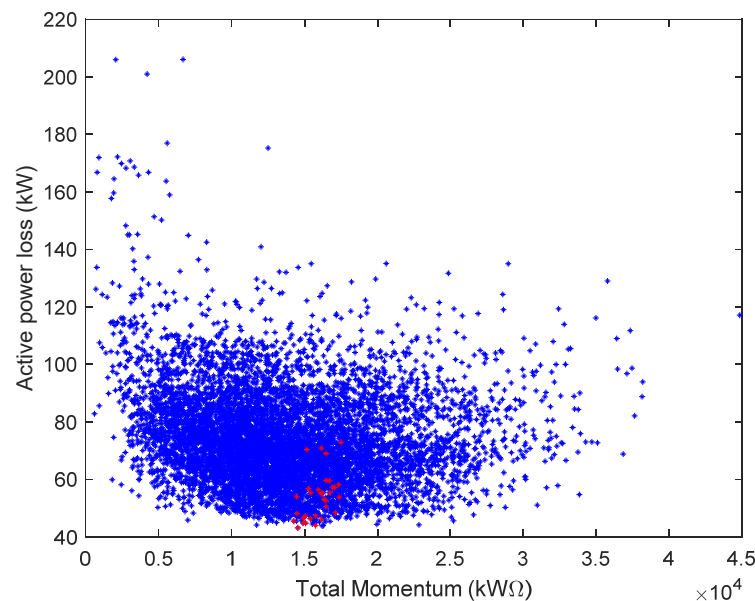


Figure 13. Variation of active power loss and the total momentum of the DGs of all possible solutions in every network structure.

10. Conclusions

In order to increase the efficiency and the reliability of a distribution network, meshed structures leveraging on SOPs are considered. Once the DGs are precisely planned and adopted into such a network, the loss reduction of the network could be further enhanced. Thus, this paper presents an approach for identifying the optimal locations and scales of DGs in an ADN with several SOPs to reduce the active power loss of the system using the PSO and VSI-based method. A generalized optimization approach is presented to evaluate the performance in terms of power loss reduction with a predefined number of DGs and SOPs in the network. In pursuance of investigating the benefits that are attributed

to the connection of adjacent feeders using SOPs, all the possible network structures with different SOP combinations are developed. Thereafter, the restructured ADNs are used to examine power loss reduction and voltage profile improvement after the integration of DGs. The findings have elaborated that the system's active power loss is affected by the sizes and the locations of the DGs and the SOP combination. When three DGs and five SOPs are added to the network, the results show that the active power loss reduction is increased by 79.5% compared to the passive network loss. In addition, a significant improvement in mean and the minimum voltages of the network is observed with the integration of DGs with SOPs.

To decide the best size and location of the DG that minimize power losses in the presence of SOPs in the network, a quantity called momentum of DG, which is the DG size into minimum impedance to the DG location from the origin, is defined. The results show that the active power loss has a U-shaped relationship with the momentum of DGs. This relationship is useful to benchmark DG integration in a network with several SOPs.

Even though the present study is in line with the state-of-the-art applications of DG sizing for the IEEE 33 bus network, it is vital to investigate the effect of load changes and reverse power flow on the optimum DG sizing as future studies. A Monte Carlo type approach could be used with the PSO optimization routine specified in this paper to investigate the effect of load changes and reverse power flow conditions.

Author Contributions: Conceptualization, J.E.; methodology, E.K.; software, E.K., and D.A.; writing—original draft preparation, E.K., J.P., J.E., and D.A.; writing—review and editing, E.K., J.P., J.E., and D.A.; visualization, E.K. and D.A.; supervision, J.P. and J.E.; project administration, J.P.; funding acquisition, J.P. All authors have read and agreed to the published version of the manuscript.

Funding: This research was funded by the Ministry of Education (MOE), Malaysia, grant number 20180117FRGS, and the APC was funded by Universiti Tenaga Nasional (UNITEN), Malaysia through J5100D4103 - BOLDREFRESH2025 - CENTRE OF EXCELLENCE.

Institutional Review Board Statement: Not applicable.

Informed Consent Statement: Not applicable.

Data Availability Statement: A publicly available dataset (IEEE 33 bus system data) was analyzed in this study.

Acknowledgments: The authors would like to thank the Ministry of Education (MOE), Malaysia, and Universiti Tenaga Nasional (UNITEN), Malaysia.

Conflicts of Interest: The authors declare no conflict of interest

Abbreviations

| | |
|-------|--------------------------------------|
| ADN | Active Distribution Network |
| BA | Bat Algorithm |
| CSCA | Chaotic Sine Cosine Algorithm |
| DG | Distributed Generators |
| GA | Genetic Algorithm |
| HSA | Harmony Search Algorithm |
| LHS | Left Hand Side |
| MINLP | Mixed Integer Non-Linear Programming |
| MOTA | Multiobjective Taguchi Approach |
| NOP | Normally Open Points |
| PSO | Particle Swarm Optimization |
| RHS | Right Hand Side |
| SOP | Soft Open Point |
| TM | Taguchi Method |
| VSC | Voltage Source Converter |
| VSI | Voltage Stability Index |

References

1. IRENA(2018). *Global Energy Transformation: A Roadmap to 2050*; International Renewable Energy Agency: Abu Dhabi, United Arab Emirates, 2018.
2. International Council on Large Electric Systems, (CIGRE Working Group 37.23). *Impact of Increasing Contribution of Dispersed Generation on the Power System-Final Report*; Electra, 1998; Available online: https://e-cigre.org/publication/ELT_199_3-impact-of-dispersed-generation-on-power-systems (accessed on 17 February 2021).
3. Guan, F.H.; Zhao, D.M.; Zhang, X.; Shan, B.T.; Liu, Z. Research on distributed generation technologies and its impacts on power system. In Proceedings of the 1st International Conference on Sustainable Power Generation and Supply, SUPERGEN '09, Nanjing, China, 6–7 April 2009; pp. 1–6.
4. Rezaee Jordehi, A. Allocation of distributed generation units in electric power systems: A review. *Renew. Sustain. Energy Rev.* **2016**, *56*, 893–905. [[CrossRef](#)]
5. Chiradeja, P.; Ramakumar, R. An approach to quantify the technical benefits of distributed generation. *IEEE Trans. Energy Convers.* **2004**, *19*, 764–773. [[CrossRef](#)]
6. Kumar, S.; Mandal, K.K.; Chakraborty, N. Optimal DG placement by multi-objective opposition based chaotic differential evolution for techno-economic analysis. *Appl. Soft Comput. J.* **2019**, *78*, 70–83. [[CrossRef](#)]
7. Nguyen, T.D.T.; Ruan, J.; Nhu Nguyen, Q.; Giang Le, N.; Tan, D.; Hu, L. Study of Economical-Technical Impacts of Distributed Generation on Medium-Voltage Grid. *TELKOMNIKA Indones. J. Electr. Eng.* **2014**, *12*, 1177–1187. [[CrossRef](#)]
8. Pesaran, H.A.M.; Huy, P.D.; Ramachandaramurthy, V.K. A review of the optimal allocation of distributed generation: Objectives, constraints, methods, and algorithms. *Renew. Sustain. Energy Rev.* **2017**, *75*, 293–312. [[CrossRef](#)]
9. Aman, M.M.; Jasmon, G.B.; Mokhlis, H.; Bakar, A.H.A. Optimal placement and sizing of a DG based on a new power stability index and line losses. *Int. J. Electr. Power Energy Syst.* **2012**, *43*, 1296–1304. [[CrossRef](#)]
10. Acharya, N.; Mahat, P.; Mithulananthan, N. An analytical approach for DG allocation in primary distribution network. *Int. J. Electr. Power Energy Syst.* **2006**, *28*, 669–678. [[CrossRef](#)]
11. Tah, A.; Das, D. Novel analytical method for the placement and sizing of distributed generation unit on distribution networks with and without considering P and PQV buses. *Int. J. Electr. Power Energy Syst.* **2016**, *78*, 401–413. [[CrossRef](#)]
12. Gözel, T.; Hocaoglu, M.H. An analytical method for the sizing and siting of distributed generators in radial systems. *Electr. Power Syst. Res.* **2009**, *79*, 912–918. [[CrossRef](#)]
13. Hung, D.Q.; Mithulananthan, N.; Bansal, R.C. Analytical expressions for DG allocation in primary distribution networks. *IEEE Trans. Energy Convers.* **2010**, *25*, 814–820. [[CrossRef](#)]
14. Kaur, S.; Kumbhar, G.; Sharma, J. A MINLP technique for optimal placement of multiple DG units in distribution systems. *Int. J. Electr. Power Energy Syst.* **2014**, *63*, 609–617. [[CrossRef](#)]
15. Mena, A.J.G.; Martín García, J.A. An efficient approach for the siting and sizing problem of distributed generation. *Int. J. Electr. Power Energy Syst.* **2015**, *69*, 167–172. [[CrossRef](#)]
16. Kashyap, M.; Mittal, A.; Kansal, S. Optimal Placement of Distributed Generation Using Genetic Algorithm Approach. In Proceedings of the Second International Conference on Microelectronics, Lecture Notes in Electrical Engineering. Computing & Communication Systems (MCCS 2017); Springer: Singapore, 2019; Volume 476, pp. 587–597.
17. Liu, W.; Luo, F.; Liu, Y.; Ding, W. Optimal siting and sizing of distributed generation based on improved nondominated sorting genetic algorithm II. *Processes* **2019**, *7*, 955. [[CrossRef](#)]
18. Abou El-Ela, A.A.; Allam, S.M.; Shatla, M.M. Maximal optimal benefits of distributed generation using genetic algorithms. *Electr. Power Syst. Res.* **2010**, *80*, 869–877. [[CrossRef](#)]
19. Dixit, M.; Kundu, P.; Jariwala, H.R. Optimal Placement and Sizing of DG in Distribution System using Artificial Bee Colony Algorithm. In Proceedings of the 2016 IEEE 6th International Conference on Power Systems (ICPS), New Delhi, India, 4–6 March 2016; pp. 1–6.
20. Suresh, M.C.V.; Edward, J.B. A hybrid algorithm based optimal placement of DG units for loss reduction in the distribution system. *Appl. Soft Comput. J.* **2020**, *91*, 106191. [[CrossRef](#)]
21. Bhullar, S.; Ghosh, S. Optimal integration of multi distributed generation sources in radial distribution networks using a hybrid algorithm. *Energies* **2018**, *11*, 628. [[CrossRef](#)]
22. Lakshmi Kumari, R.V.S.; Nagesh Kumar, G.V.; Siva Nagaraju, S.; Babita Jain, M. Optimal sizing of distributed generation using particle swarm optimization. In Proceedings of the 2017 International Conference on Intelligent Computing, Instrumentation and Control Technologies, ICICICT 2017, Kannur, India, 6–7 July 2017; Volume 2018, pp. 499–505.
23. Karunarathne, E.; Pasupuleti, J.; Ekanayake, J.; Almeida, D. Network loss reduction and voltage improvement by optimal placement and sizing of distributed generators with active and reactive power injection using fine-tuned pso. *Indones. J. Electr. Eng. Comput. Sci.* **2021**, *21*, 647–656. [[CrossRef](#)]
24. Karunarathne, E.; Pasupuleti, J.; Ekanayake, J.; Almeida, D. Comprehensive learning particle swarm optimization for sizing and placement of distributed generation for network loss reduction. *Indones. J. Electr. Eng. Comput. Sci.* **2020**, *20*, 16–23. [[CrossRef](#)]
25. Karunarathne, E.; Pasupuleti, J.; Ekanayake, J.; Almeida, D. Multi-Leader Particle Swarm Optimization for Optimal Planning of Distributed Generation. In Proceedings of the 2020 IEEE Student Conference on Research and Development (SCORED), Batu Pahat, Johor, Malaysia, 27–29 September 2020; pp. 96–101.

26. Cao, W.; Wu, J.; Jenkins, N. Feeder load balancing in MV distribution networks using soft normally-open points. In Proceedings of the IEEE PES Innovative Smart Grid Technologies, Europe, Istanbul, Turkey, 12–15 October 2014; pp. 1–6.
27. Cao, W.; Wu, J.; Jenkins, N.; Wang, C.; Green, T. Benefits analysis of Soft Open Points for electrical distribution network operation. *Appl. Energy* **2016**, *165*, 36–47. [[CrossRef](#)]
28. Long, C.; Wu, J.; Thomas, L.; Jenkins, N. Optimal operation of soft open points in medium voltage electrical distribution networks with distributed generation. *Appl. Energy* **2016**, *184*, 427–437. [[CrossRef](#)]
29. Cao, W.; Wu, J.; Jenkins, N.; Wang, C.; Green, T. Operating principle of Soft Open Points for electrical distribution network operation. *Appl. Energy* **2016**, *164*, 245–257. [[CrossRef](#)]
30. Qi, Q.; Wu, J.; Long, C. Multi-objective operation optimization of an electrical distribution network with soft open point. *Appl. Energy* **2017**, *208*, 734–744. [[CrossRef](#)]
31. Li, P.; Ji, H.; Yu, H.; Zhao, J.; Wang, C.; Song, G.; Wu, J. Combined decentralized and local voltage control strategy of soft open points in active distribution networks. *Appl. Energy* **2019**, *241*, 613–624. [[CrossRef](#)]
32. Bloemink, J.M.; Green, T.C. Increasing distributed generation penetration using soft normally-open points. In Proceedings of the IEEE PES General Meeting, Providence, RI, USA, 25–29 July 2010; pp. 1–8.
33. Modarresi, J.; Gholipour, E.; Khodabakhshian, A. A comprehensive review of the voltage stability indices. *Renew. Sustain. Energy Rev.* **2016**, *63*, 1–12. [[CrossRef](#)]
34. Karunarithne, E.; Pasupuleti, J.; Ekanayake, J.; Almeida, D. Optimal Placement and Sizing of DGs in Distribution Networks Using MLPSO Algorithm. *Energies* **2020**, *13*, 6185. [[CrossRef](#)]
35. Abdmouleh, Z.; Gastli, A.; Ben-Brahim, L.; Haouari, M.; Al-Emadi, N.A. Review of optimization techniques applied for the integration of distributed generation from renewable energy sources. *Renew. Energy* **2017**, *113*, 266–280. [[CrossRef](#)]
36. Gkaidatzis, P.A.; Doukas, D.I.; Labridis, D.P.; Bouhouras, A.S. Comparative analysis of heuristic techniques applied to ODGP. In Proceedings of the 2017 17th IEEE International Conference on Environment and Electrical Engineering and 2017 1st IEEE Industrial and Commercial Power Systems Europe, IEEEIC/I and CPS Europe 2017, Milan, Italy, 6–9 June 2017.
37. Kennedy, J.; Eberhart, R. Particle Swarm Optimization Proceedings. IEEE International Conference. *Proc. ICNN'95 Int. Conf. Neural Networks* **1995**, *11*, 111–117.
38. Baran, M.E.; Wu, F.F. Network reconfiguration in distribution systems for loss reduction and load balancing. *IEEE Trans. Power Deliv.* **1989**, *4*, 1401–1407. [[CrossRef](#)]
39. Sgouras, K.I.; Bouhouras, A.S.; Gkaidatzis, P.A.; Doukas, D.I.; Labridis, D.P. Impact of reverse power flow on the optimal distributed generation placement problem. *IET Gener. Transm. Distrib.* **2017**, *11*, 4626–4632. [[CrossRef](#)]
40. Selim, A.; Kamel, S.; Jurado, F. Efficient optimization technique for multiple DG allocation in distribution networks. *Appl. Soft Comput. J.* **2020**, *86*, 105938. [[CrossRef](#)]
41. Meena, N.K.; Swarnkar, A.; Gupta, N.; Niazi, K.R. Multi-objective Taguchi approach for optimal DG integration in distribution systems. *IET Gener. Transm. Distrib.* **2017**, *11*, 2418–2428. [[CrossRef](#)]
42. Sudabattula, S.S.; Kowsalya, M. Optimal allocation of solar based distributed generators in distribution system using Bat algorithm. *Perspect. Sci.* **2016**, *8*, 270–272. [[CrossRef](#)]
43. Rao, R.S.; Ravindra, K.; Satish, K.; Narasimham, S.V.L. Power loss minimization in distribution system using network reconfiguration in the presence of distributed generation. *IEEE Trans. Power Syst.* **2013**, *28*, 317–325. [[CrossRef](#)]